



Contents lists available at ScienceDirect

Journal of the Mechanical Behavior of Biomedical Materials

journal homepage: <http://www.elsevier.com/locate/jmbbm>

# Adhesion, biological corrosion resistance and biotribological properties of carbon films deposited on MAO coated Ti substrates

Wei Yang<sup>a,\*</sup>, Yu Gao<sup>a</sup>, Peng Guo<sup>b</sup>, Dapeng Xu<sup>a</sup>, Lin Hu<sup>a</sup>, Aiying Wang<sup>b,\*\*</sup><sup>a</sup> School of Materials Science and Chemical Engineering, Xi'an Technological University, Xi'an, 710032, China<sup>b</sup> Key Laboratory of Marine New Materials and Related Technology, Zhejiang Key Laboratory of Marine Materials and Protection Technology, Ningbo Institute of Material Technology & Engineering, Chinese Academy of Sciences, Ningbo, 315201, China

## ARTICLE INFO

## Keywords:

Pure Ti  
Carbon films  
Micro arc oxidation  
Adhesion  
In vitro properties

## ABSTRACT

A thin diamond-like carbon (DLC) film, a graphite-like carbon (GLC) film and a thick diamond-like carbon (PE-DLC) film are deposited on the micro arc oxidation (MAO) coated pure titanium substrates using a hybrid ion beam deposition system, magnetron sputtering and plasma enhanced chemical vapor deposition, respectively. The microstructure, adhesion, biological corrosion resistance and biotribological properties were determined. The results showed that the three duplex coatings presented uneven surface features and increased binding force. The binding force of the duplex coatings was strongly affected by the bonding strength between the MAO coating and Ti substrate. Although the roughness Ra of the three duplex coatings was high, their friction coefficients were small (under 0.22) in the SBF solution. The MAO/DLC and MAO/GLC coatings showed an excellent tribological behavior and corrosion resistance in the SBF solution.

## 1. Introduction

Titanium alloys have some advantages of high strength, strong corrosion resistance, good biocompatibility and non-toxicity, using in many fields of industries (Hussein et al., 2016; Wang et al., 2017; Chen et al., 2017). Especially, pure titanium is commonly used in different applications due to its good structural properties, but its poor corrosion resistance and tribological property seriously affect the safety and restrict its usage areas (Xu et al., 2018; Kao et al., 2018). Therefore, different surface modifications on titanium material surfaces are applied to enhance its properties (Yu et al., 2018; Janson et al., 2019; Huang et al., 2009).

Microarc oxidation (MAO), also called plasma electrolytic oxidation (PEO), is a technique to grow a ceramic coating on Al, Mg or Ti substrates utilizing micro arc discharge generated by dielectric breakdown (Durdu et al., 2018; Yang et al., 2018a, 2018b; Liu et al., 2016; Li et al., 2017). The obtained TiO<sub>2</sub> coating presents high hardness, high wear resistance, and good adhesion with substrate, etc. (Koshuro et al., 2018). Nonetheless, as the MAO coated Ti materials as dental and orthopedic implants are exposed to body fluid, they undergo sliding wear and corrosion, resulting in a poor wear resistance due to a porous structure,

which limits the application of titanium implants (Fazel et al., 2015). Carbon films, such as diamond-like carbon (DLC) and graphite-like carbon (GLC), have been widely used in biomedical applications due to their biocompatibility, anti-corrosion, and chemical inertness (He et al., 2015; Du et al., 2014; Alexeev et al., 2018). Many techniques, such as physical vapor deposition (PVD) and chemical vapor deposition (CVD), are being developed to deposit carbon films. More importantly, it has been proved that a porous MAO coating as an interlayer of carbon films can increase the mechanical interlocking and mechanical property on the substrate (Yang et al., 2013). Finally, with the help of the lubrication and chemical inertness of top carbon films, the biological protection performance of titanium can be greatly improved.

In this paper, a MAO coating was prepared on the titanium substrate as the interlayer of the carbon films, and then hybrid-beam magnetron sputtering was used to prepare a DLC film, a GLC film was prepared by magnetic filter cathodic arc composite sputtering, and a thicker DLC film was prepared by plasma enhanced chemical vapor deposition (PE-DLC). The performance of three types of carbon films on the MAO coated substrates will be different in the simulated body fluid. Actually, the corrosion process of these composite coatings could be accelerated by the corrosion medium of the SBF solution in the electrochemical test.

\* Corresponding author.

\*\* Corresponding author.

E-mail addresses: [yangwei\\_smx@163.com](mailto:yangwei_smx@163.com) (W. Yang), [aywang@nimte.ac.cn](mailto:aywang@nimte.ac.cn) (A. Wang).<https://doi.org/10.1016/j.jmbbm.2019.103448>

Received 20 August 2019; Received in revised form 18 September 2019; Accepted 23 September 2019

Available online 23 September 2019

1751-6161/© 2019 Elsevier Ltd. All rights reserved.

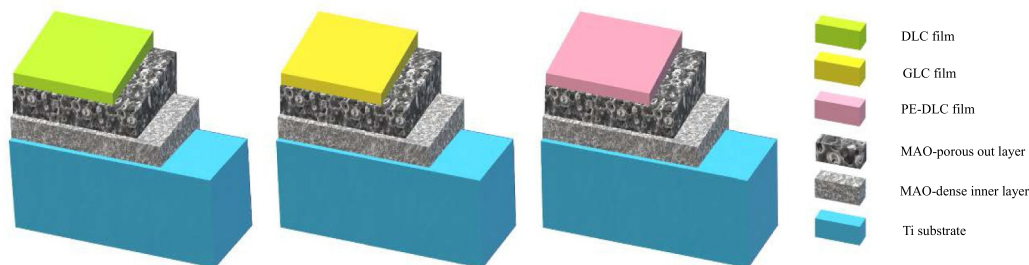


Fig. 1. Structural schematic diagram of three duplex films on Ti substrates.

Corrosion from the SBF solution could accelerate wear of the composite coatings; but the SBF solution could form a liquid film at the wear interface, which was helpful to reduce wear. So the purpose of this paper was to systematically evaluate the microstructure, wear resistance, in vitro corrosion resistance and tribological behavior of the three carbon films on the MAO treated titanium, which could provide experimental support for the screening of such composite coatings. Based on the above comparison of different carbon films on the MAO coated Ti substrates, this newly designed coating/substrate system could provide an experimental support for biological application of titanium and its alloys in this study.

## 2. Experimental

TA2 pure titanium specimens had a diameter of 15 mm and a thickness of 5 mm. The specimens were ultrasonically cleaned in acetone and ethanol. The MAO coatings were prepared using JHMAO-60 micro arc oxidation equipment (made by Xi'an University of Technology, China). The appropriate electrical parameters were as follows: constant voltage, 450 V; frequency, 500 Hz; duty cycle, 8%; processing time, 6 min. The electrolyte for the MAO treatment was sodium silicate ( $\text{Na}_2\text{SiO}_3 \cdot 9\text{H}_2\text{O}$ , 10.0 g/L). Prior to deposition for the DLC, GLC and PE-DLC films, the MAO coated Ti substrates were sputter-cleaned for 5 min using Ar with a bias voltage of  $-100$  V. The base pressure was evacuated to a vacuum of  $1.3 \times 10^{-2}$  Pa. The DLC film was deposited by a hybrid ion beam deposition system (Dai et al., 2010). Hydrocarbon gas ( $\text{C}_2\text{H}_2$ , 38 sccm) was introduced into the linear ion source with 0.2 A to obtain the hydrocarbon ions for the DLC deposition for 40 min under a negative bias of  $-100$  V. The GLC film was grown by filtered cathodic vacuum arc

(FCVA) deposition, and the Ar sputtering gas with 50 sccm was supplied to the graphite cathode target for C sputtering with a sputtering current of 3.0 A under a negative bias of  $-200$  V for 120 min. The PE-DLC films were prepared by the plasma enhanced chemical vapor deposition (PECVD) system using Hydrocarbon gas ( $\text{C}_2\text{H}_2$ , 100 sccm) under a working pressure of  $2.0 \times 10^3$  Pa for 60 min. The pulse width and pulse frequency were  $1.1 \mu\text{s}$  and 350 Hz. The structural schematic diagram of the three duplex films is shown in Fig. 1.

The thicknesses of the DLC, GLC and PE-DLC films were measured by the Alpha-step IQ profilers, and the values were 688.3 nm, 696.5 nm and 1644.2 nm, respectively. The surface morphologies of the MAO/DLC, MAO/GLC and MAO/PE-DLC coatings were characterized by scanning electron microscopy (SEM) and atomic force microscopy (AFM). The element distribution of the wear scars was detected by energy dispersive spectrometer (EDS). The phases of the three top carbon films before and after the friction tests were analyzed by using Raman scattering spectroscopy in air at room temperature (Ferrari and Robertson, 2000). The adhesion of the three duplex coatings to the Ti substrates was assessed by a scratch tester performed on a rockwell diamond indenter with a conical tip of 0.2 mm in radius. The normal load of the indenter was linearly ramped from the minimum load (1 N) to the maximum load (30 N) during scratching. The scratch length was 3.00 mm and the scratch speed was 1.5 mm/min. The mechanical properties of the three duplex coatings were evaluated by a nanoindentation tester with the maximum indentation depths kept under the values of 10 % of the total thickness for each film. The tribological behaviors of the MAO/DLC, MAO/GLC and MAO/PE-DLC coated samples were measured on a UMT tribolab friction tester in the SBF solution at room temperature. During the tests, a 2 N contact load, speed 150 mm/min and friction time 1200 s

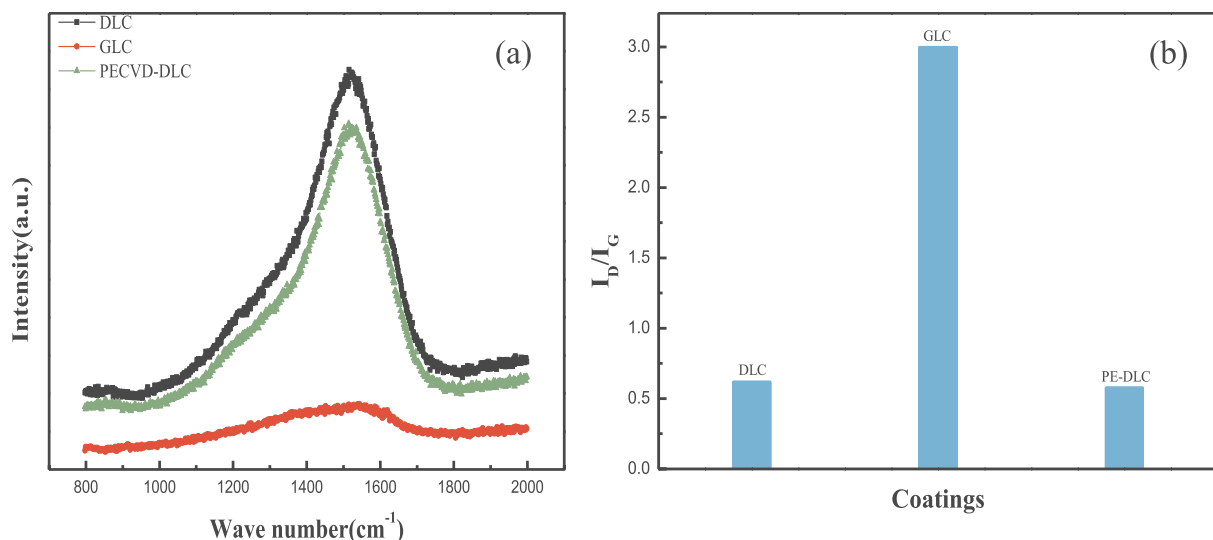
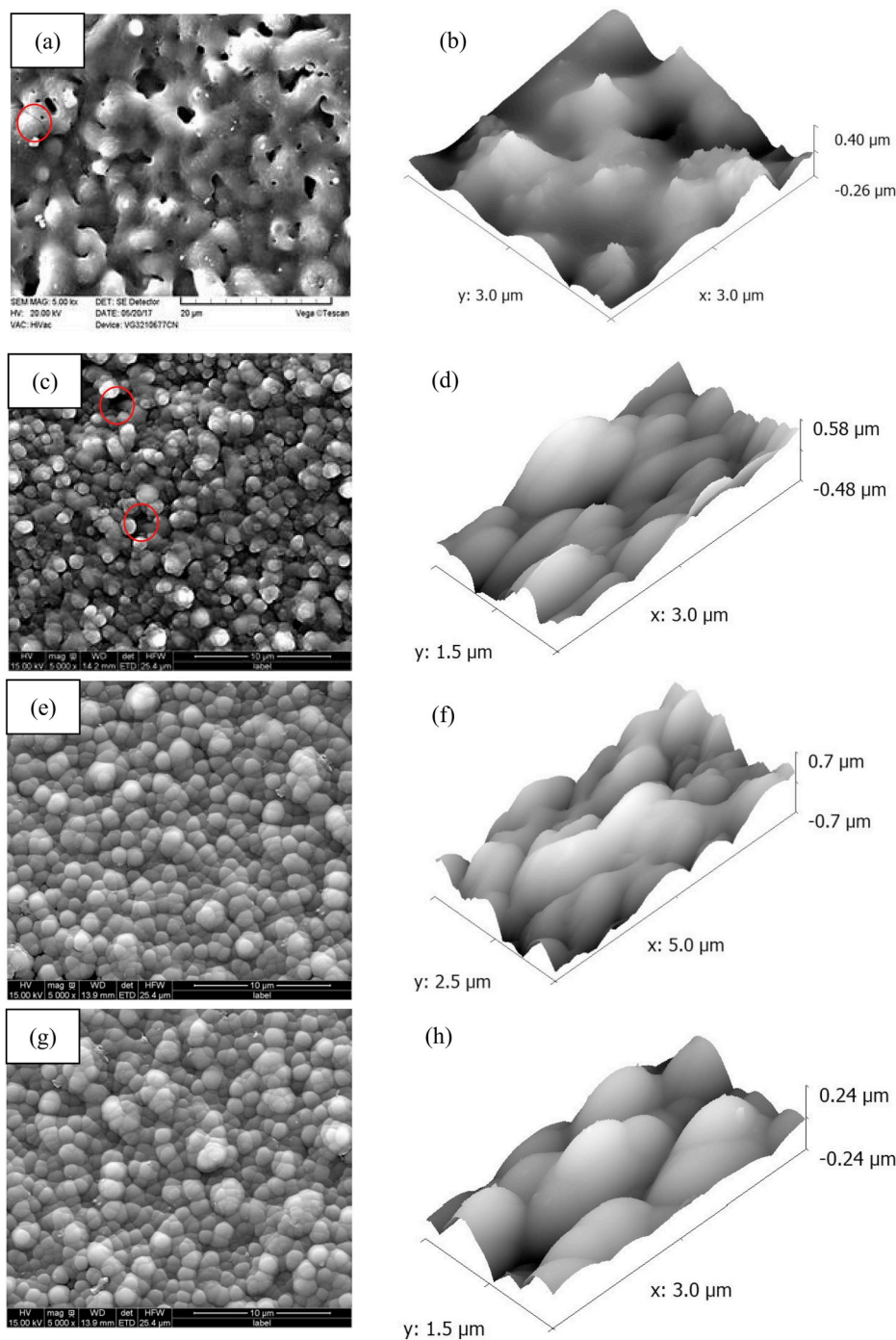


Fig. 2. (a) Raman spectra and (b)  $I_D/I_G$  of DLC, GLC and PE-DLC films on Si substrates.



**Fig. 3.** Surface SEM and AFM morphologies of four coatings, (a) and (b) MAO, (c) and (d) MAO/DLC, (e) and (f) MAO/GLC, (g) and (h) MAO/PE-DLC.

were applied on the coated samples with a  $\text{Al}_2\text{O}_3$  ball. The corrosion resistance of the three coated pure Ti samples was evaluated by electrochemical test in the SBF solution (Yang et al., 2019). Before each measurement, the open circuit potential (OCP) of samples was monitored for 5 min to stabilize the surface condition. The scanning speed is 5 mV/s. A 64 bit system-zview software was used to fit and calculate the characterization parameters of electrochemical corrosion.

### 3. Results and discussion

Raman spectra of the DLC, GLC and PE-DLC films are shown in Fig. 2. According to the intensity ratio of D peak to G peak ( $I_D/I_G$ ), the  $\text{sp}^2/\text{sp}^3$  ratio of the carbon films can be characterized (Savchenko et al., 2018;

Robertson, 2002). It was noted that the G peak position shifted towards high wave number and the  $I_D/I_G$  ratio also dramatically increased in the GLC film compared with the DLC and PE-DLC films, implying a high graphitization degree. For the DLC and PE-DLC films, although the thickness of the two films was quite different, the G peak position and  $I_D/I_G$  value was similar, indicating a high diamond degree.

Fig. 3 shows the surface SEM and AFM morphologies of the MAO, MAO/DLC, MAO/GLC and MAO/PE-DLC coatings on the Ti substrates. Fig. 3 (a) and (b) showed that the MAO coating had some sharp bumps, showing an obvious volcanic-like morphology, and there were some micropores with different apertures and microcracks (Region marked by red color) due to the high temperature and high pressure produced by micro arc discharge (Xu et al., 2017). As a result, this coating had the

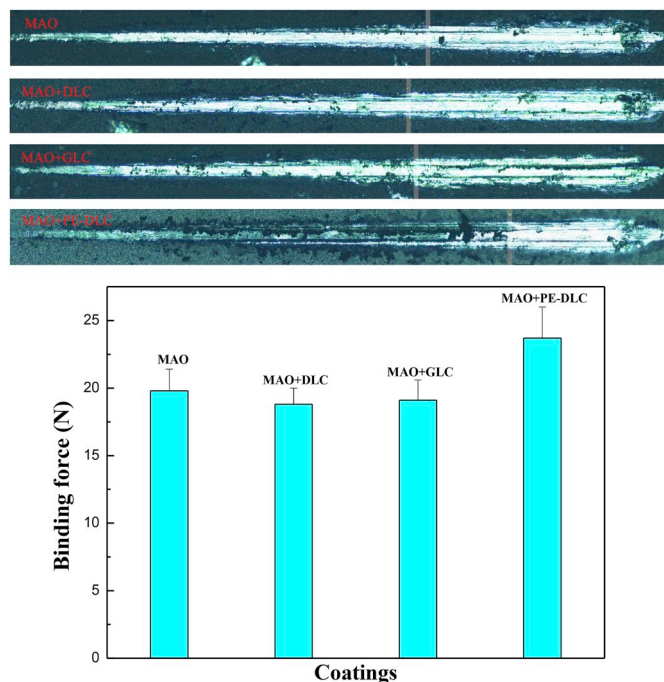


Fig. 4. Scratch morphologies and critical loads of four coatings on pure Ti substrates.

maximum roughness 931 (nm). In the case of the MAO/DLC coating, shown in Fig. 3 (c), it could be obtained that this duplex coating was not uniform and the micropores was covered by the top DLC film (Region marked by red color), resulting in a decreased aperture. Compared with the MAO/DLC coating, the MAO/GLC and MAO/PE-DLC coatings presented characteristics of cellular bulges, shown in Fig. 3 (e) and (g). The micropores of the MAO coating were not found and these two duplex coatings showed a compact microstructure. The AFM results showed that, as deposition of carbon film on the MAO coatings, the obtained MAO/DLC, MAO/GLC and MAO/PE-DLC duplex coatings presented much smoother than that of MAO monolayer, showing low roughness, and the Ra values of MAO/DLC, MAO/GLC and MAO/PE-DLC coatings were 164 nm, 211 nm and 157 nm, respectively. Furthermore, these three duplex coatings had some cellular bulges, and the larger the carbon film thickness was, the larger the shape of cellular bulges was. Interestingly, the Ra of MAO/GLC (211 nm) was higher than that of MAO/DLC (164 nm) and MAO/PE-DLC (157 nm), and the reason was that, firstly, the thicknesses of the DLC, GLC and PE-DLC films were 688.3 nm, 696.5 nm and 1644.2 nm, respectively. So the sealing effect of the top DLC and GLC films on the MAO coatings is not as good as PE-DLC film. As a result, the Ra of the MAO/PE-DLC coating was smallest. Secondly, for the MAO/DLC and MAO/GLC two coatings, it was observed that some large cellular bulges were on the MAO/GLC coating, which resulted in a higher Ra value than the MAO/DLC coating.

To obtain the high adhesion is one of the major purposes for the DLC or GLC protective films on Ti substrates. Fig. 4 showed the scratch morphologies and critical loads of the four coated samples in the scratch test in this study. The results showed that, the MAO/PE-DLC duplex coating exhibited higher critical loads than the other three coatings deposited on the Ti substrates, but the MAO, MAO/DLC and MAO/GLC coatings had a similar critical load value (Nearly 20 N). So it could be speculated that the critical loads of the MAO/DLC and MAO/GLC duplex coatings were determined by the metallurgical bonding at the interface created by MAO treatment as the carbon film was thin. The critical loads of the MAO/PE-DLC duplex coatings had the maximum value (23.7 N) among the four coatings, which might be attributable to the obvious resistance for the top thick carbon film. As a result, the duplex MAO/PE-

Table 1

Hardness (H), elastic modulus (E), H/E values and electrochemical results of MAO/DLC, MAO/GLC and MAO/PE-DLC coated Ti substrates.

Coatings	H/GPa	E/GPa	H/E	$E_{\text{corr}}/V$	$i_{\text{corr}}/(A/cm^2)$
substrates	3.72	123.4	0.028	-0.109	$2.38 \times 10^{-9}$
MAO + DLC	16.72	184.14	0.091	-0.018	$4.88 \times 10^{-9}$
MAO + GLC	7.70	100.06	0.077	-0.081	$1.51 \times 10^{-8}$
MAO + PE-DLC	15.94	176.62	0.090	-0.109	$2.38 \times 10^{-9}$

DLC coating exhibited the highest critical load, which was very useful to improve the tribological behavior of the coated sample.

The hardness and elastic modulus of Ti substrate, MAO/DLC, MAO/GLC and MAO/PE-DLC coatings were measured by using CSM method. To eliminate the influence of the Ti substrate on the measured hardness and Young's modulus, the hardness and Young's modulus values in the indentation depth range of 10% coating thickness were averaged. Table 1 illustrates the hardness (H), elastic modulus (E) and the ratio of hardness to modulus of elasticity (H/E) values of the four coatings deposited on the Ti substrates. As shown, the hardness of the three duplex coatings was higher than that of the Ti substrate, and the hardness of the MAO/DLC and MAO/PE-DLC coatings was much higher than that of MAO/GLC coating, which was related to  $sp^3/sp^2$  bonding ratio. The elastic modulus is an index to measure the degree of elastic deformation of materials. The larger the E value is, the more difficult the elastic deformation is (Yang et al., 2018c). As a result, the MAO/GLC coating had a low E value compared with the MAO/DLC and MAO/PE-DLC coatings due to the layered structure of GLC film. It was known that the H/E values indicated the relative variation of the elastic deformation and plastic deformation of the coatings under compressive stress. So, a high H/E value indicated that the plough wear resistance of the coating was excellent, resulting in a low wear rate. Obviously, the MAO/DLC and MAO/PE-DLC coatings might have excellent tribological behavior.

Fig. 5 (a) presents the friction coefficient of the three coated Ti substrate against sliding time against an Al<sub>2</sub>O<sub>3</sub> ball in the SBF solution. It was found that as the wear time prolonged, the friction coefficient fluctuated significantly, but it kept between 0.205 and 0.220. In particular, the MAO/GLC coating had a low friction coefficient compared with the MAO/DLC and MAO/PE-DLC coatings. It has been reported that the friction coefficient of the DLC film deposited on Ti substrate could be kept below 0.10, which was much lower than that of MAO/DLC, MAO/GLC and MAO/PE-DLC coatings (Kang et al., 2015). It could be speculated that a high and fluctuated friction coefficient of the three coatings was related to an increased Ra values of the duplex coatings affected by the porous morphology of MAO interlayer. Furthermore, the friction coefficients of the three duplex coatings did not increase abruptly during the friction tests, which indicated that the top carbon film was not peeled off from the MAO coating and the carbon film still played a very good role in protecting the Ti substrate. Raman spectra and  $I_D/I_G$  values of MAO/DLC, MAO/GLC and MAO/PE-DLC coatings and the grinding ball before and after friction tests are shown in Fig. 5 (b). It was found that the  $I_D/I_G$  value for the MAO/DLC coating was almost no change before and after friction test, indicating that the stability of this duplex coating during friction process was helpful to improve the tribological behavior. Furthermore, it was obtained that there was a formation of carbon transfer film with a diamond-like structure in the grinding ball. For the MAO/GLC coating, the  $I_D/I_G$  value significantly decreased after friction test, indicating an enhanced degree of diamond. But a carbon transfer film was not found in the grinding ball due to an excellent lubrication of the top MAO/GLC coating. Similar to the MAO/DLC film, although the top DLC film was increased, the  $I_D/I_G$  value for the MAO/PE-DLC film was also almost no change before and after friction test and there was still a formation of carbon transfer film with a diamond-like structure in the grinding ball.

The wear scars and the debris composition of the duplex coatings

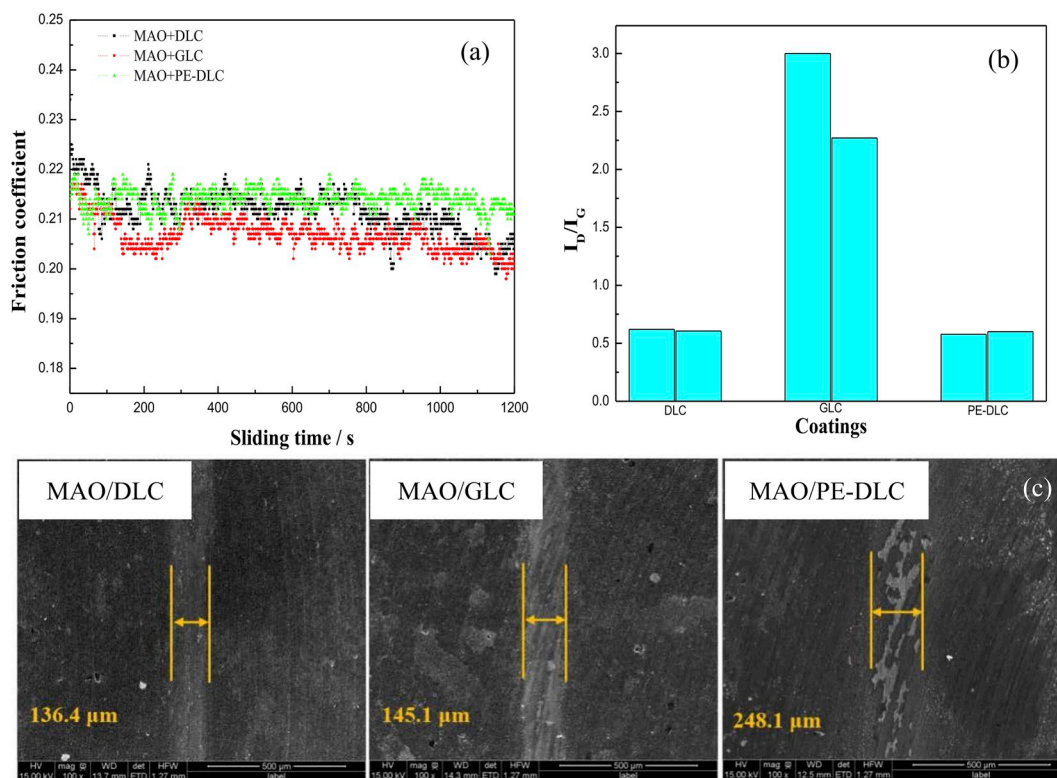


Fig. 5. Evaluation of tribological behavior for three coatings on Ti substrates in SBF solution, (a) Friction curves, (b)  $I_p/I_G$  before and after friction, (c) Wear tracks.

Table 2

Composition at wear tracks of MAO/DLC, MAO/GLC and MAO/PE-DLC coated Ti.

Coatings	C, at%	O, at%	Na, at%	Al, at%	Si, at%	Ti, at%
MAO/DLC	79.66	4.19	0.18	0.18	5.53	10.26
MAO/GLC	72.16	6.30	0.22	0.26	7.24	13.82
MAO/PE-DLC	81.16	3.14	0.14	0.42	5.00	10.13

after friction tests were analyzed by SEM and EDS, shown in Fig. 5 (c) and Table 2. The results showed that the width of wear scars of the MAO/DLC, MAO/GLC and MAO/PE-DLC coated samples was 136.4  $\mu\text{m}$ , 145.1  $\mu\text{m}$ , and 248.1  $\mu\text{m}$ , respectively. It was observed that the wear scars of MAO/DLC and MAO/GLC coated Ti substrates was shallow and narrow, and the Ti substrate was still protected by the two coatings. The width of wear scar of the MAO/PE-DLC coated Ti substrate was much larger than that of the MAO/DLC and MAO/GLC coated samples. Especially, the MAO/GLC coating had the low friction coefficient among the three coatings, but the width of wear scar of the MAO/GLC coating was not smallest, which was attributed to its low hardness, H/E value and reduced graphitization during the wear process. The wear scar width of MAO/PE-DLC duplex coating was much higher than that of the MAO/DLC coating due to significant differences in surface morphologies. It was observed that the top DLC film was thin compared with the PE-DLC film, and the porous interface of the MAO/DLC coating was helpful to store SBF solution and form liquid film for improving its wear resistance. The dense surface structure with amount of cellular bulges of the MAO/PE-DLC coating resulted in the increase of friction coefficient, and so it had lowest wear scar width. Besides, there were some white attachments on the wear scar of the MAO/PE-DLC coating. The EDS results showed that the detected a large number of C element on the wear tracks of the MAO/DLC, MAO/GLC and MAO/PE-DLC coated samples denoted that the three duplex coatings were survived during all the sliding. In other aspect, much less of O was detected on the wear tracks of the three duplex coatings, which indicated that high-

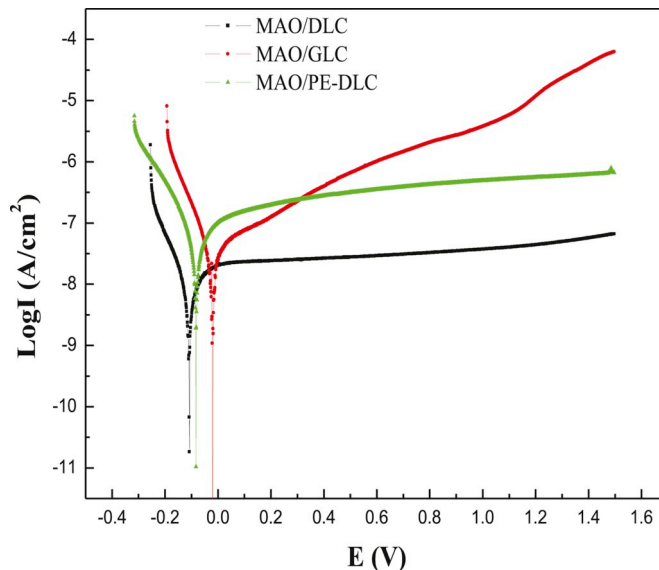


Fig. 6. Polarization curves of three coated samples in SBF solution.

temperature oxidation process during the sliding process was observably restrained by the top carbon film. A very small amount of Al and Na elements from the SBF solution were found on the wear tracks, which could affect their tribological behavior. Furthermore, it was noted that more C elements from the top carbon film and less of Ti element from the substrate and Si element from the MAO electrolyte were found on the MAO/PE-DLC coating, which indicated that, although the wear scar width of the MAO/PE-DLC coating was large and the friction coefficient fluctuated obviously, this duplex coating still had a good protective effect on the Ti substrates.

The polarization curves of MAO/DLC, MAO/GLC and MAO/PE-DLC

coated Ti samples in the SBF solution are shown in Fig. 6. Corrosion potential and corrosion current density obtained from Fig. 6 by Tafel analysis are shown in Table 1. Based on these electrochemical parameters, it was found that the corrosion current densities of the MAO/DLC and MAO/GLC coatings were almost low one order of magnitude compared with the MAO/PE-DLC coating, indicating an enhanced corrosion resistance. It was confusing that although the MAO/PE-DLC coating with improved binding force and thick top carbon films, the corrosion resistance and tribological behavior were worse. The reason might be that the corrosion resistance of the coating-substrate depended on the top carbon film, and a significant increase in the thickness of the carbon film might result in its internal stress enhancement and bond angle distortion. Besides, more compact surface morphology of MAO/PE-DLC was not helpful to the formation of lubricating liquid film in the SBF solution. Furthermore, the corrosion potential of the MAO/GLC coated sample was markedly higher than that of the MAO/DLC and MAO/PE-DLC coated samples, indicating the duplex coating was not easy to corrode. So it was obtained that the MAO/GLC coating had more excellent corrosion resistance in this test.

#### 4. Conclusions

- 1) The DLC, GLC and PE-DLC films were deposited on the MAO coated Ti substrates. These three duplex coatings presented uneven surface morphologies, and the microporous defects of the MAO coatings were obviously reduced. As a result, the MAO/PE-DLC showed the highest critical loads (23.7 N).
- 2) Although the friction coefficients of the three duplex coatings were high and fluctuated during the friction process in the SBF solution, they still had low friction coefficients (0.205 and 0.220). Especially, the MAO/DLC coating had the lowest wear scar width (136.4  $\mu\text{m}$ ) among the three duplex coatings due to a formation of carbon transfer film with a diamond-like structure in the grinding ball.
- 3) The corrosion current densities of MAO/DLC and MAO/GLC coatings were almost low one order of magnitude compared with the MAO/PE-DLC coating in the SBF solution. Besides, the MAO/GLC coating had the highest corrosion potential ( $-0.018\text{ V}$ ), indicating that the MAO/GLC coating had more excellent corrosion resistance in this test.

#### Conflicts of interest

We declare that we have no financial and personal relationships with other people or organizations that can inappropriately influence our work, there is no professional or other personal interest of any nature or kind in any product, service and/or company that could be construed as influencing the position presented in, or the review of, the manuscript entitled, "Adhesion, biological corrosion resistance and biotribological properties of carbon films deposited on MAO coated Ti substrates".

#### Acknowledgment

The authors gratefully acknowledge the financial support of the Key Research and Development Plan of Shaanxi Province-industrial Project (2018GY-127), Key Laboratory of Marine Materials and Related Technologies, CAS (2019K02) and Shaanxi Provincial Education Department Program (18JK0394). The authors would like to express their special thanks to Dr. H. Li, Y. Liu, and W.J. Hou (at Ningbo Institute of Material Technology & Engineering, Chinese Academy of Sciences) for their help in characterization of coatings for this paper.

#### References

Alexeev, A.M., Ismagilov, R.R., Obratsov, A.N., 2018. Structural and morphological peculiarities of needle-like diamond crystallites obtained by chemical vapor deposition. *Diam. Relat. Mater.* 87, 261–266.

- Chen, Y.H., Kent, D.M., Bermingham, M., Dehghan-Manshadi, A., Dargusch, M., 2017. Manufacturing of biocompatible porous titanium scaffolds using a novel spherical sugar pellet space holder. *Mater. Lett.* 195, 92–95.
- Dai, W., Wu, G.S., Wang, A.Y., 2010. Preparation, characterization and properties of Cr-incorporated DLC films on magnesium alloy. *Diam. Relat. Mater.* 19, 1307–1315.
- Du, D.X., Liu, D.X., Ye, Z.Y., Zhang, X.H., Li, F.Q., Zhou, Z.Q., Yu, L., 2014. Fretting wear and fretting fatigue behaviors of diamond-like carbon and graphite-like carbon films deposited on Ti-6Al-4V alloy. *Appl. Surf. Sci.* 313, 462–469.
- Durdu, S., Aktug, S.L., Korkmaz, K., Yalcin, E., Aktas, S., 2018. Fabrication, characterization and in vitro properties of silver-incorporated TiO<sub>2</sub> coatings on titanium by thermal evaporation and micro-arc oxidation. *Surf. Coat. Technol.* 352, 600–608.
- Fazel, M., Salimijazi, H.R., Golozar, M.A., Garsivaz jazi, M.R., 2015. A comparison of corrosion, tribocorrosion and electrochemical impedance properties of pure Ti and Ti6Al4V alloy treated by micro-arc oxidation process. *Appl. Surf. Sci.* 324, 751–756.
- Ferrari, A., Robertson, J., 2000. Interpretation of Raman spectra of disordered and amorphous carbon. *Phys. Rev. B* 61, 14095–14107.
- He, D.Q., Zheng, S.X., Pu, J.B., Zhang, G.A., Hu, L.T., 2015. Improving tribological properties of titanium alloys by combining laser surface texturing and diamond-like carbon film. *Tribol. Int.* 82, 20–27.
- Huang, C.F., Cheng, H.C., Liu, C.M., Chen, C.C., Ou, K.L., 2009. Microstructure and phase transition of biocompatible titanium oxide film on titanium by plasma discharging. *J. Alloy. Compd.* 476, 683–688.
- Hussein, A.H., Gepreel, Mohamed A.H., Gouda, M.K., Hefnawy, Ahmad M., Kandil, Sherif H., 2016. Biocompatibility of new Ti-Nb-Ta base alloys. *Mater. Sci. Eng. C* 61, 574–578.
- Janson, O., Gururaj, S., Pujari-Palmer, S., Ott, M.K., Strømme, M., Engqvist, H., Welch, K., 2019. Titanium surface modification to enhance antibacterial and bioactive properties while retaining biocompatibility. *Mater. Sci. Eng. C* 96, 272–279.
- Kang, S., Lim, H.P., Lee, K., 2015. Effects of TiCN interlayer on bonding characteristics and mechanical properties of DLC-coated Ti-6Al-4V ELI alloy. *Int. J. Refract. Metals Hard Mater.* 53, 13–16.
- Kao, W.H., Su, Y.L., Horng, J.H., Chang, C.Y., 2018. Tribological, electrochemical and biocompatibility properties of Ti6Al4V alloy produced by selective laser melting method and then processed using gas nitriding, CN or Ti-C:H coating treatments. *Surf. Coat. Technol.* 350, 172–187.
- Koshuro, V., Fomin, A., Rodionov, I., 2018. Composition, structure and mechanical properties of metal oxide coatings produced on titanium using plasma spraying and modified by micro-arc oxidation. *Ceram. Int.* 44, 12593–12599.
- Li, Q.B., Yang, W.B., Liu, C.C., Wang, D.A., Liang, J., 2017. Correlations between the growth mechanism and properties of micro-arc oxidation coatings on titanium alloy: Effects of electrolytes. *Surf. Coat. Technol.* 316, 162–170.
- Liu, S.M., Li, B.E., Liang, C.Y., Wang, H.S., Qiao, Z.X., 2016. Formation mechanism and adhesive strength of a hydroxyapatite/TiO<sub>2</sub> composite coating on a titanium surface prepared by micro-arc oxidation. *Appl. Surf. Sci.* 362, 109–114.
- Robertson, J., 2002. Diamond-like amorphous carbon. *Mater. Sci. Eng. R* 37, 129–281.
- Savchenko, D., Vorlíček, V., Prokhorov, A., Kalabukhova, E., Lančok, J., Jelínek, M., 2018. Raman and EPR spectroscopic studies of chromium-doped diamond-like carbon films. *Diam. Relat. Mater.* 83, 30–37.
- Wang, Xiaoyan, Qu, Zeming, Li, Jianjun, Zhang, Erlin, 2017. Comparison study on the solution-based surface biomodification of titanium: Surface characteristics and cell biocompatibility. *Surf. Coat. Technol.* 329, 109–119.
- Xu, J.L., Xiao, Q.F., Mei, D.D., Tong, Y.X., Zheng, Y.F., Li, L., Zhong, Z.C., 2017. Microstructure, corrosion resistance and formation mechanism of alumina micro-arc oxidation coatings on sintered NdFeB permanent magnets. *Surf. Coat. Technol.* 309, 621–627.
- Xu, W., Lu, X., Wang, L.N., Shi, Z.M., Lv, S.M., Qian, M., Qu, X.H., 2018. Mechanical properties, in vitro corrosion resistance and biocompatibility of metal injection molded Ti-12Mo alloy for dental applications. *J. Mech. Behav. Biomed. Mater.* 88, 534–547.
- Yang, W., Zhang, D., Deng, Z.N., Ke, P.L., Wang, A.Y., 2013. Microstructure and tribological behavior of self-lubricating (Si<sub>3</sub>N<sub>4</sub>)-DLC/MAO coatings on AZ80 magnesium substrate. *Acta Metall. Sin.* 26, 693–698.
- Yang, W., Xu, D.P., Wang, J.L., Yao, X.F., Chen, J., 2018. Microstructure and corrosion resistance of micro arc oxidation plus electrostatic powder spraying composite coating on magnesium alloy. *Corros. Sci.* 136, 174–179.
- Yang, W., Xu, D.P., Guo, Q.Q., Chen, T., Chen, J., 2018. Influence of electrolyte composition on microstructure and properties of coatings formed on pure Ti substrate by micro arc oxidation. *Surf. Coat. Technol.* 349, 522–528.
- Yang, P.F., Nie, X.T., Zhao, D.D., Wang, Z., Ren, L., Xu, H.Y., Rittweger, J., Shang, P., 2018. Deformation regimes of collagen fibrils in cortical bone revealed by in situ morphology and elastic modulus observations under mechanical loading. *J. Mech. Behav. Biomed. Mater.* 79, 115–121.
- Yang, W., Xu, D.P., Gao, Y., Hu, L., Ke, P.L., Chen, J., 2019. Microstructure, adhesion, in vitro corrosion resistance and tribological behavior of (Si<sub>3</sub>N<sub>4</sub>)-DLC coated pure Ti. *Diam. Relat. Mater.* 92, 109–116.
- Yu, S.Z., Li, Z.H., Han, L.W., Zhao, Y.T., Fu, T., 2018. Biocompatible MgO film on titanium substrate prepared by sol-gel method. *Rare Metal Mater. Eng.* 47, 2663–2667.